



Original Contribution

Contribution of glutathione status to oxidant-induced mitochondrial DNA damage in colonic epithelial cells

Magdalena L. Circu^a, Mary P. Moyer^b, Lynn Harrison^a, Tak Yee Aw^{a,*}^a Department of Molecular and Cellular Physiology, Louisiana State University Health Sciences Center, Shreveport, LA 71130, USA^b INCELL Corporation, San Antonio, TX 78249, USA

ARTICLE INFO

Article history:

Received 16 January 2009

Revised 20 July 2009

Accepted 26 July 2009

Available online 6 August 2009

Keywords:

Mitochondrial DNA damage

Glutathione

Glutathione redox state

Colon cells

Menadione

Mitochondrial base excision repair

Free radicals

ABSTRACT

Although oxidative stress induces mitochondrial DNA (mtDNA) damage, a role for redox in modulating mtDNA oxidation and repair is relatively unexplored. This study examines the contribution of cellular glutathione (GSH) redox status to menadione (MQ)-induced mtDNA damage and postoxidant mtDNA recovery in a nontransformed NCM460 colonic cell line. We show that MQ caused dose-dependent increases in mtDNA damage that were blunted by *N*-acetylcysteine, a thiol antioxidant. Damage to mtDNA paralleled mitochondrial protein disulfide formation and glutathione disulfide increases in the cytosol and mitochondria and was exacerbated by inhibition of GSH synthesis in accordance with decreased cytosolic and mitochondrial GSH. Blockade of mitochondrial GSH (mtGSH) transport potentiated mtDNA damage, which was prevented by overexpression of the oxoglutarate mtGSH carrier, underscoring a link between mtGSH and mtDNA responsiveness to oxidative stress. The removal of MQ posttreatment elicited mtDNA recovery to basal levels by 4 h, indicating complete repair. Notably, mtDNA recovery was preceded by restored cytosolic and mtGSH levels at 2 h, suggesting a connection between the maintenance of cell GSH and effective mtDNA repair. The MQ-induced dose-dependent increase in mtDNA damage was attenuated by overexpressing mitochondrial 8-oxoguanine DNA glycosylase (Ogg1), consistent with 7,8-dihydro-8-oxoguanine being a major oxidative mtDNA lesion. Collectively, the results show that oxidative mtDNA damage in colonic cells is highly responsive to the mtGSH status and that postoxidant mtDNA recovery may also be GSH sensitive.

© 2009 Elsevier Inc. All rights reserved.

Mitochondria are major players in the regulation of cellular processes, including oxidant-mediated apoptotic signaling. An important mitochondrial component that is highly vulnerable to oxidative damage is the mitochondrial DNA (mtDNA) [1–3], owing to its open circular structure, lack of histone protection, and proximity to the mitochondrial electron transport chain, a main source of reactive oxygen species (ROS) [2,3]. The mitochondrial genome encodes several hydrophobic components of the respiratory chain belonging to complexes I, II, and IV and ATP synthase that is essential for oxidative phosphorylation. MtDNA damage will decrease the gene expression of these key respiratory proteins [4]. An enhanced ROS production from consequent disruption in the electron flow creates a vicious cycle of mitochondrial dysfunction that ultimately results in cell apoptosis [5]. The findings that oxidative mtDNA damage can induce cell apoptosis [6] have spurred much interest in understanding the factors that influence oxidative mtDNA damage and its repair. At steady state, the extent of mtDNA damage would be determined by the efficiency of its repair. The mitochondrial base excision repair (mtBER)

system plays a central role in the removal of oxidized base damage. Specific DNA glycosylases release the damaged bases, generating abasic (AP) sites that are further cleaved by AP endonucleases [7,8]. Of importance, the 8-oxoguanine DNA glycosylase (Ogg1) recognizes and removes 7,8-dihydro-8-oxoguanine (8-oxoG) [9–11], a biologically relevant oxidative lesion induced by mitochondrially derived ROS [12]. A decrease in mitochondrial Ogg1 has been shown to correlate with mitochondria-initiated apoptosis [13].

The mitochondrial glutathione (mtGSH) status is expected to play a quantitative role in the degree of mtDNA damage, given that ROS-induced oxidative stress is typically associated with altered redox balance. MtGSH maintains mitochondrial integrity via its versatile role in oxidant reduction, electrophile conjugation, and preservation of protein–SH and is an integral component of the mitochondrial redox cycle in the elimination of ROS that arise as by-products of aerobic respiration and enhanced mitochondrial dysfunction. Early studies have shown that loss of mtGSH is an important factor in oxidative vulnerability [14], implicating the significance of this redox compartment in cell survival. A link between loss of mtGSH and cytotoxicity was previously observed for aromatic hydrocarbons [15], hypoxia [16], *tert*-butylhydroperoxide [17], ethanol intoxication [18], and acetaminophen [19]. Our recent studies have demonstrated that

* Corresponding author. Fax: +1 318 675 4217.

E-mail address: taw@lsuhsc.edu (T.Y. Aw).

decreased mtGSH is a key contributor to the sensitization of colonic cells to menadione-induced apoptosis [20]. Within the mitochondrial matrix, steady-state GSH concentration can be maintained by the reduction of glutathione disulfide (GSSG), as catalyzed by the flavoenzyme glutathione reductase, or achieved by uptake from the cytosol through specific carriers located in the inner mitochondrial membrane. In liver and kidney, the organic anion carriers 2-oxoglutarate (OGC) and dicarboxylate (DIC) have been characterized as effective transporters of mtGSH [21–23]. Chemical or genetic modulation of these transporter functions was shown to alter the intra-mtGSH status [23].

In this study, we have investigated the relationship between mtGSH and oxidative mtDNA damage caused by menadione (2-methyl-1,4-naphthoquinone; MQ), a redox cycling quinone that we recently found to induce significant mtGSH oxidation and colonic cell apoptosis [20]. The contribution of mtGSH to MQ-mediated mtDNA damage was examined in the nonmalignant NCM460 or malignant HT-29 human colonic epithelial cell lines, using pharmacologic and genetic approaches to manipulate mtGSH transport and mitochondrial matrix (mt-matrix) GSH status. Our results demonstrate that MQ dose-dependently elicited mtDNA damage that was exacerbated by inhibition of cellular GSH synthesis and prevented by *N*-acetylcysteine. Significantly, oxidative mtDNA damage was exaggerated by attenuated mtGSH transport in association with increased mtGSSG, and postoxidant recovery of mtDNA was preceded by restored cytosolic and mtGSH status. Taken together, these results show that the extent of mtDNA damage and the capacity for repair are influenced by the cellular GSH redox state, particularly that of mtGSH.

Materials and methods

The following chemicals were obtained from Sigma Chemicals (St. Louis, MO, USA): menadione sodium bisulfite, *N*-acetylcysteine (NAC), EDTA, EGTA, sucrose, dithiothreitol, 2,4-dinitrofluorobenzene, iodoacetic acid, glutathione (GSH and GSSG), butylmalonic acid (BM), phenylsuccinic acid (PS), calf thymus DNA, Tris base, sodium dodecyl sulfate, sodium chloride, sodium hydroxide, and sodium citrate. M3:10 medium was acquired from INCELL Corp. (San Antonio, TX, USA). Antibiotic/antimycotic, McCoy's medium, L-glutamine, and trypsin were obtained from GIBCO (Grand Island, NY, USA). Fetal bovine serum (FBS) was acquired from Atlanta Biologicals (Norcross, GA, USA). Protein dye assay kit and Zeta-Probe GT blotting membranes were obtained from Bio-Rad (Hercules, CA, USA). DNA extraction kit was obtained from Qiagen (Valencia, CA, USA). DNase-free RNase and *Xho*I enzymes were purchased from Roche Applied Bioscience (Indianapolis, IN, USA). λ DNA *Hind*III marker, *Taq* polymerase, deoxynucleotides, and PCR buffer were from Promega (Madison, WI, USA). All other reagents were of analytical grade and were purchased from local sources.

Cell culture and nucleofection

Cell lines

NCM460 is an immortalized and nonmalignant human colonic epithelial cell line [24] that was generated by Dr. Mary Moyer (INCELL Corp.). The NCM460 cell line was derived from the transverse colon of a human donor and exhibits characteristics similar to those of primary cultures of cells isolated from the same region [25]. NCM460 cells were cultured in M3:10 medium in a 5% CO₂/95% air humidified environment at 37 °C. A single stock of NCM460 cells was obtained from INCELL and expanded, which we have designated as passage 0; subsequent cell expansions for either freezing back or experiments were designated consecutively as passage 1, 2, 3, etc. In this study, NCM460 cell passages 75–85 were used in all experiments. The human colon epithelial cell line HT-29, originally isolated from a colon adenocarcinoma of a female Caucasian, was purchased from the

American Type Culture Collection (Manassas, VA, USA). HT-29 cells were grown in McCoy's medium supplemented with 10% fetal bovine serum and 2 mM glutamine. In recent studies, we found that the responses of cellular GSH/GSSG to oxidants and nonoxidants were similar in HT-29 and NCM460 cells [20,26].

Nucleofection and generation of stable colon cell lines

Compared to NCM460 cells, HT-29 cells were easy to transfect and exhibited a high percentage and yield of transfection. Hence, HT-29 cells were used to generate stable cell lines that overexpress specific mitochondria-targeted proteins. To overexpress the mitochondrial OGC, cells were nucleofected with either pcDNA 3.1 (vector control) or the expression vector containing wild-type rat OGC (pcDNA 3.1/rOGC-WT) (gifts from Dr. Lawrence Lash, Wayne State University School of Medicine, Detroit, MI, USA). To overexpress the mitochondrial Ogg1, cells were nucleofected with either pcDNA3.neo (vector control) or pcDNA3 plasmid carrying the mitochondrial targeting sequence-Ogg1 cDNA (a gift from Dr. Susan LeDoux, University of South Alabama, Mobile, AL, USA). Nucleofection was performed with the Nucleofector II system (Amaxa GmbH, Cologne, Germany) according to the manufacturer's protocol (Amaxa Biosystems). Briefly, cells were passaged 3 days before nucleofection and grown to 70% confluency. Cells were harvested by trypsinization and 1×10^6 cells were mixed with 100 μ l of nucleofector solution and 2 μ g plasmid DNA. Samples were transferred into cuvettes and nucleofected using program W-17. Cells were resuspended in growth medium and allowed to grow for 2–3 days. After being replated at a population density of 5×10^3 /cm², the cells were grown in culture medium containing 800 μ g/ml G418 (Invitrogen, San Diego, CA, USA) to select for cells that had integrated the plasmid DNA into their genome. The

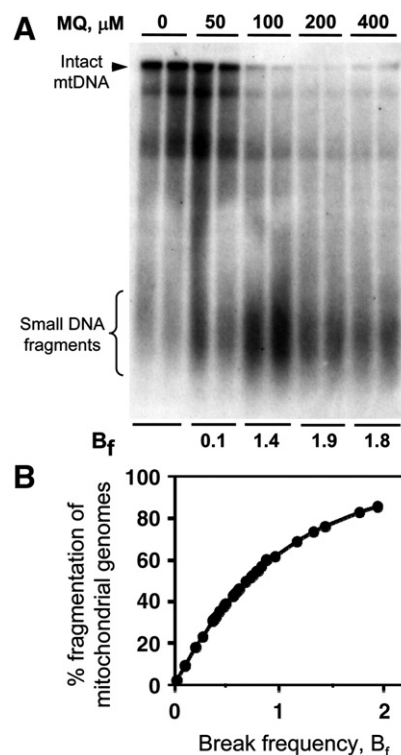


Fig. 1. MQ dose-dependently increases mtDNA damage. (A) NCM460 cells were exposed to 50, 100, 200, and 400 μ M MQ for 1 h; thereafter, the cells were harvested and processed for quantitative Southern analyses using a human mtDNA-specific probe as described under **Materials and methods**. Intact mtDNA (arrowhead) ran at the top of the 0.6% agarose alkaline gels, whereas damaged mtDNA was represented by small DNA fragments and is expressed as strand break frequency (B_f) [31]. DNA samples were run in duplicates for untreated controls and each MQ dose. One representative of three gels is shown. (B) Relationship between percentage fragmentation of mitochondrial genomes and B_f generated using Southern analyses from Figs. 1, 3, 4, 5, 7, and 8.

cell medium was changed every 2 days until single colonies formed. The colonies were isolated, maintained in 500 $\mu\text{g}/\text{ml}$ G418, and individually expanded to form the respective cell lines. Genomic DNA was prepared using the Qiapm DNA blood mini kit (Qiagen) and tested for vector DNA incorporation in the genome by PCR. The expression of the recombinant proteins was verified in mitochondrial protein extracts by Western blot analyses.

Cell incubation and digitonin fractionation

Incubation protocols

Preincubation with chemical agents. Colonic cells ($5 \times 10^6/\text{ml}$) were plated in T25 flasks in complete medium 1 day before the experiment. The next day, the medium was changed to FBS- and phenol red-free Dulbecco's modified Eagle medium (DMEM). Preincubations with BM/PS or NAC were according to the following conditions: BM/PS, 20 mM each, 1 h; NAC, 2 mM, 30 min. For buthionine sulfoximine (BSO) experiments, cells were seeded at $3 \times 10^6/\text{ml}$ and the next day were pretreated with 5 or 20 μM BSO for another 24 h in complete medium. Thereafter, the medium was replaced by FBS- and phenol red-free DMEM.

Cell incubations with MQ. At the end of the respective preexposure times, cell incubations with MQ were performed in one of two ways. In studies of mitochondrial and cytosolic GSH redox status, cells were

harvested by trypsinization and resuspended in Dulbecco PBS at a concentration of $2 \times 10^6/\text{ml}$. Incubations were then performed in cells in suspension with 100 or 200 μM MQ at 37 °C for various times in rotating round-bottom flasks in a Rotavap system [27]. In experiments to test the effects of NAC, BM/PS, or BSO, these agents were present throughout the incubation. Studies on mtDNA and GSH recovery were conducted using 200 μM MQ; this 200 μM dose was selected to ensure a higher level of mtDNA damage such that a larger difference between mtDNA damage and recovery can be quantified. In dose-dependent experiments, MQ concentrations of 50, 100, 200, and 400 μM were used. At designated times, cell aliquots were removed and subjected to digitonin fractionation (see below) for determination of GSH contents in the cytosol and mitochondria.

Digitonin fractionation

The cytosolic and mitochondrial fractions were obtained using digitonin fractionation [28]. Briefly, digitonin fractionation was performed in 1.5-ml Eppendorf tubes containing, from the bottom: 100 μl 10% trichloroacetic acid (TCA), 500 μl of silicone oil/mineral oil mixture (4/1, v/v), and 100 μl of digitonin solution (1.2 mg/ml PBS). A 500- μl aliquot of cell suspension was added to the digitonin top layer and then centrifuged at 10,000 g for 5 min. The supernatant was removed and the silicone/mineral oil mixture was aspirated. The supernatant and TCA layers were collected and stored at -80 °C until analyses. Samples of these fractions, representing the cytosolic and mitochondrial compartments, respectively, were assayed for GSH and

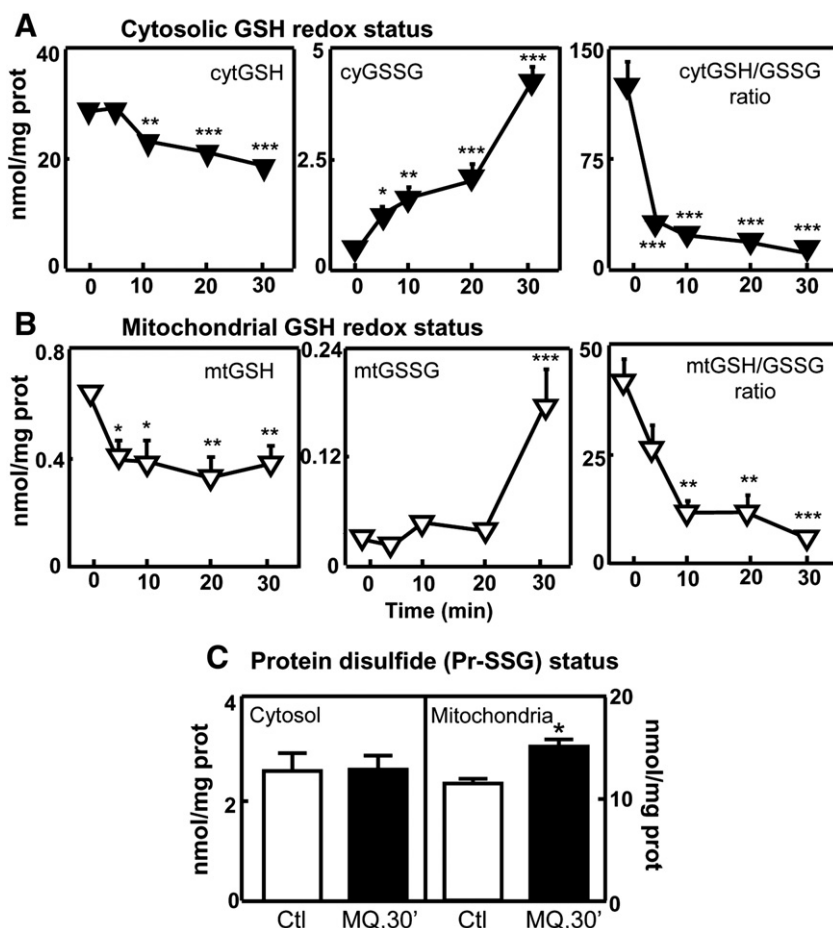


Fig. 2. Kinetics of MQ-induced changes in cytosolic and mitochondrial GSH, GSSG, and protein disulfide. NCM460 cells were treated with 100 μM MQ for 0–30 min and cytosolic and mitochondrial fractions were separated by digitonin fractionation. The contents of GSH, GSSG, and protein-SGG in each compartment were determined as described under [Materials and methods](#). (A, B) Cytosolic and mitochondrial GSH redox status, respectively. Concentrations of GSH and GSSG are expressed as nmol/mg protein and presented as means \pm SE for four separate experiments performed in duplicates. Statistical differences between 0 min and other time points are * $P < 0.05$; ** $P < 0.01$; *** $P < 0.001$. (C) Protein-SGG content. Left and right are cytosolic and mitochondrial protein-SGG, respectively. Results are expressed as nmol/mg protein and presented as means \pm SE for three separate experiments performed in duplicates. * $P < 0.05$ versus untreated control.

GSSG, as well as protein disulfides (protein–SSG). To verify clean separation of the mitochondrial and cytosolic compartments, aliquots of each fraction were routinely assayed for the activities of their respective enzyme markers, viz., glutamate dehydrogenase and lactate dehydrogenase as previously described [20].

Determination of GSH, GSSG, and protein–SSG

GSH/GSSG measurements

Soluble GSH and GSSG were determined in TCA supernatants by high-performance liquid chromatography (HPLC) according to a modified method of Reed et al., as we previously described [29,30]. Experimentally, samples were derivatized with 6 mM iodoacetic acid and 1% 2,4-dinitrofluorobenzene to yield the *S*-carboxymethyl and 2,4-dinitrophenyl derivatives, respectively. Separation of GSH and GSSG derivatives was performed on a 250 × 4.6-mm Alltech Lichrosorb NH₂ 10- μ m column using a Shimadzu HPLC system. GSH and GSSG contents were determined in mitochondrial and cytosolic compartments collected by digitonin fractionation (see above) and were expressed as nmol/mg protein.

Protein–SSG

Protein-bound disulfide was measured in TCA-insoluble proteins as we previously described [29]. Briefly, the mitochondrial insoluble proteins obtained from the TCA layer after digitonin fractionation were dissolved in 0.1 M NaOH and neutralized to pH 8. Samples were mixed with phosphate buffer (1.5 mM KH₂PO₄, 6.36 mM K₂HPO₄, 1.57 mM EDTA) containing 2 mM 5,5'-dithiobis(2-nitrobenzoic acid) and incubated for 15 min at room temperature. Total protein–SH and protein–SSG were determined colorimetrically at 410 nm; protein–SSG was calculated from the difference of absorbance before and after addition of saturated *N*-ethylmaleimide solution. Protein–SSG concentrations were expressed as nmol/mg protein.

Protein assay

Protein concentrations were determined using the Bio-Rad protein assay kit (Bio-Rad) according to the manufacturer's protocol.

DNA extraction and quantitative Southern analyses of mtDNA damage

After treatment with the various chemical agents, cells were washed twice with cold PBS, harvested by scraping, and processed for quantitative Southern analyses. Total DNA was extracted with a QIAamp DNA mini kit according to the manufacturer's protocol (Qiagen) and the mtDNA was visualized using a modified quantitative Southern blot method of Dobson et al. [31]. In brief, DNA was ethanol precipitated, treated with DNase-free RNase (1 μ g/ml), and digested with restriction endonuclease *Xho*I (5 U/ μ g DNA) overnight at 37 °C to linearize the mtDNA. DNA samples were ethanol precipitated, dissolved in TE buffer (10 mM Tris, 1 mM EDTA, pH 8), and quantified fluorometrically in a Hoefer DyNA Quant200 fluorometer. Restriction-digested DNA samples (2 μ g) were heated at 70 °C for 15 min, cooled, and treated with 0.1 N NaOH at 37 °C for 20 min to generate single-stranded DNA. The digested DNA samples were resolved on 0.6% agarose alkaline gels at 1.5 V for 12–16 h in an alkaline buffer containing 23 mM NaOH and 1 mM EDTA. The next day, DNA was transferred under vacuum to a Zeta-Probe GT nylon membrane and cross-linked using a Model 2400 Stratalinker (Stratagene, La Jolla, CA, USA) at 120,000 μ J/cm². The membrane was hybridized with a ³²P-labeled human mtDNA-specific probe at 56 °C in a Model 131000 hybridization oven (Boekel Scientific, Feasterville, PA, USA). The mtDNA probe was a 672-bp PCR DNA fragment of the mitochondrial ATP synthase F0 subunit 6 generated from HeLa genomic DNA. The following primers were used to generate the probe: 5'-CACAACTAACCTCCTCG-3' and 5'-CTTTTGGACAGGTGGTG-3'. The mtDNA band intensity for each sample was quantified using a phosphorimager

(Molecular Dynamics, Sunnyvale, CA, USA) and mtDNA damage was expressed as strand break frequency (B_f) determined from the negative natural log of the band intensities of treated and control samples as previously described [32]. The B_f value is an arbitrary number calculated using a Poisson distribution and reflects the extent of oxidant-induced mtDNA damage over control [32]. In our studies, we found that B_f values between 0.09 and 1 are essentially linearly correlated with percentage fragmentation of total mitochondrial genomes, calculated as $[1 - (E/C)] \times 100$, where *E* and *C* represent band intensities of treated and control DNA samples, respectively ($R^2 = 0.99$; Fig. 1B). From this relationship, a B_f of 1 corresponded to ~60% fragmentation of total mitochondrial genome, consistent with substantial damage.

Statistical analysis

Results are expressed as means \pm SE. Data were analyzed using a one-way ANOVA with Bonferroni corrections for multiple comparisons. *P* values of <0.05 were considered statistically significant.

Results

MQ-induced mtDNA damage and post-MQ mtDNA recovery: relationship to cytosolic and mitochondrial GSH redox and protein disulfide status

Fig. 1 shows the effects of MQ exposure on mtDNA damage in NCM460 cells. Treatment of cells with MQ ranging from 50 to 400 μ M caused dose-dependent increases in small DNA fragments that paralleled the decreases in intact mtDNA, consistent with mtDNA damage. DNA B_f of 0.1, 1.4, 1.9, and 1.8, corresponding to 9, 76, 86, and 83% fragmentation of total mitochondrial genomes (Figs. 1A and 1B), were elicited by 50, 100, 200, and 400 μ M MQ, respectively. Because MQ exhibits redox cycling properties, the results suggest that MQ induces colonic mtDNA damage by an oxidative, redox-dependent mechanism. To examine the extent to which cellular redox status was altered, we quantified GSH and GSSG contents in the cytosolic and

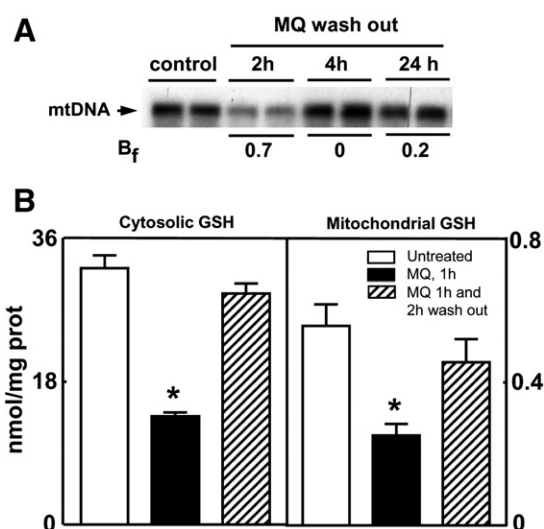


Fig. 3. Restoration of mitochondrial and cytosolic GSH precedes post-MQ recovery of mtDNA integrity. (A) NCM460 cells were exposed to 200 μ M MQ for 1 h, and thereafter the incubation medium was replaced with fresh MQ-free medium. At 2, 4, and 24 h, cells were harvested for genomic DNA extraction and mtDNA was determined by quantitative Southern blot analyses as described under Materials and methods. DNA samples were run in duplicates and one representative of three gels is shown. mtDNA damage is expressed as strand B_f . (B) In parallel experiments, GSH contents in cytosolic (left) and mitochondrial (right) compartments were determined. GSH concentrations are expressed as nmol/mg protein and presented as means \pm SE of three separate experiments performed in duplicates. **P* < 0.05 versus untreated control.

mitochondrial compartments. Fig. 2A shows that MQ caused significant time-dependent decreases in cytosolic GSH (10–30 min), with parallel increases in GSSG beginning at as early as 5 min. This resulted in a shift in the GSH-to-GSSG ratio in favor of GSSG at all time points. MQ similarly elicited time-dependent decreases in mtGSH (10–30 min), increases in mtGSSG (30 min), and overall decreases in the mtGSH-to-mtGSSG ratio (10–30 min) (Fig. 2B). These results indicate that MQ-induced mtDNA damage in NCM460 cells is associated with both cytosolic and mitochondrial GSH redox imbalance. In contrast, MQ caused significant protein–SSG formation only in the mitochondria, not in the cytosol (Fig. 2C), indicating that MQ mediated preferential oxidation of mitochondrial protein thiols and suggesting that overall losses of mtGSH and protein thiol redox balance could be important contributors to oxidative mtDNA damage.

The kinetic relationship between cytosolic and mitochondrial GSH and post-MQ recovery of mtDNA integrity was determined after 1 h exposure to 200 μM MQ followed by 2 to 24 h MQ washout. This level of MQ exposure resulted in mtDNA B_f of 1.9 (86% fragmentation, Fig. 1). The results in Fig. 3A show that MQ-induced mtDNA damage remained significant at 2 h after removal of MQ. By 4 h, the levels of mtDNA returned to pre-MQ values and were maintained at 24 h. This finding suggests that removal of the oxidative challenge resulted in full recovery of baseline mtDNA within hours, consistent with an efficient repair mechanism after oxidative stress [31,33]. GSH levels were

determined in parallel and the results show that 1 h treatment with MQ induced significant GSH decreases in the mitochondrial and cytosolic pools, and removal of MQ restored GSH to preoxidant levels at 2 h in both compartments (Fig. 3B). Notably, the kinetics of GSH restoration preceded full recovery of mtDNA by approximately 2 h (Fig. 3A), suggesting the interesting possibility that a restored GSH status could facilitate the repair of oxidative mtDNA lesions.

Attenuation of MQ-induced mtDNA damage by NAC and overexpression of mtOgg1

To further explore the relationship between cellular GSH redox status and oxidative mtDNA damage, cells were pretreated with NAC, a thiol antioxidant. Fig. 4A shows that at 100 μM , MQ induced significant damage to mtDNA ($B_f=0.7$, corresponding to 51% fragmentation, Fig. 1B) that was attenuated by 2 mM NAC pretreatment ($B_f=0.09$, corresponding to 9% fragmentation, Fig. 1B), validating that mtDNA susceptibility to oxidative challenge is redox sensitive. The same dose of NAC was equally effective in protecting against greater oxidative mtDNA damage induced by 200 μM MQ ($B_f=1.3$ versus 0.02; Fig. 4A). Measurements of GSH/GSSG revealed that, regardless of dose, MQ induced similar mtGSH decreases and mtGSSG increases at 30 min with resultant severe mitochondrial GSH/GSSG redox imbalance (Fig. 4B). Cells pretreated with NAC

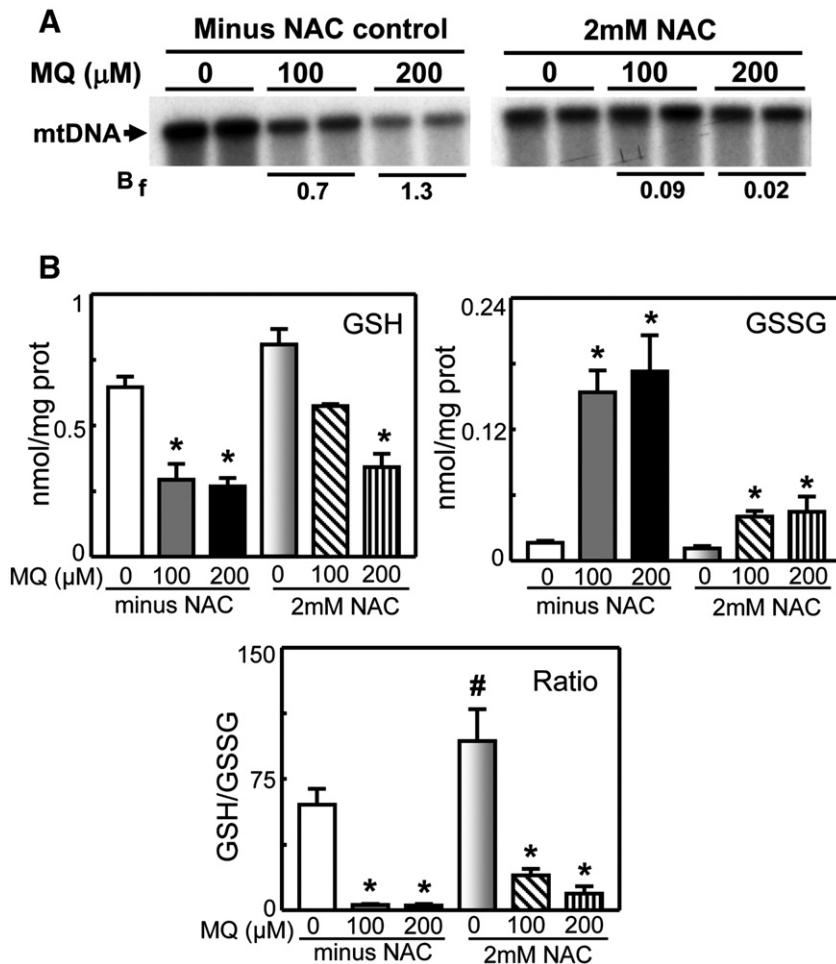


Fig. 4. Effects of *N*-acetylcysteine on MQ-induced mtDNA damage and the relationship to mitochondrial GSH/GSSG redox status. (A) NCM460 cells were plated in T25 flasks and pretreated with 2 mM NAC (30 min) before MQ exposure at 100 and 200 μM for 30 min. Total DNA was extracted and mtDNA was quantified by Southern blot analysis as described under Materials and methods. mtDNA damage is expressed as strand B_f . One representative of three gels is shown. (B) In parallel experiments, mitochondrial fractions were obtained after selective permeabilization of plasma membrane with digitonin as described under Materials and methods. Mt-matrix GSH and GSSG concentrations were determined. Top left, mtGSH; top right, mtGSSG; bottom, mtGSH-to-mtGSSG ratio. Results are expressed as means \pm SE of three separate experiments performed in duplicates. * $P < 0.001$ versus controls (i.e., respective 0 μM MQ minus or plus NAC); # $P < 0.001$ versus 0 μM MQ minus NAC.

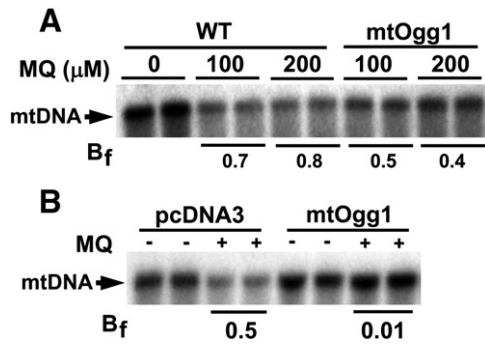


Fig. 5. Overexpression of mtOgg1 protects against MQ-induced mtDNA damage. HT-29 WT cells as well as clones overexpressing the empty pcDNA3 vector or mtOgg1 ((A) 1.5-fold above WT and vector control and (B) 2.7-fold above vector control) were exposed to MQ (100 μM (A, B) and 200 μM (A)) for 1 h. Genomic DNA was extracted and mtDNA was determined by quantitative Southern blot analyses. DNA samples were run in duplicates and mtDNA damage is expressed as strand B_f. One representative of three gels is shown. In (A), band intensities of intact mtDNA were similar for WT and pcDNA3 vector controls (data not shown). Similarly, intact mtDNA band intensities of WT (data not shown) were similar to those of pcDNA3 vector controls in (B).

exhibited higher baseline mtGSH levels that were decreased only at 200 μM MQ. Importantly, NAC pretreatment significantly attenuated MQ-induced mtGSSG increases (Fig. 4B, top right), but did not fully restore baseline mitochondrial GSH/GSSG balance (Fig. 4B, bottom), suggesting that the blunting of mtDNA damage by NAC was associated with its capacity to decrease mtGSSG per se.

To test whether 8-oxoG is a biologically important mtDNA lesion [34] induced by MQ, HT-29 cells were stably transfected with the mitochondria-targeted DNA glycosylase Ogg1 and exposed to MQ. The results show that the extent of mtDNA damage induced by MQ at 100 and 200 μM in wild type (WT) ($B_f = 0.7$ and 0.8 , respectively, Fig. 5A) and vector control (data not shown) was markedly attenuated in mtOgg1-overexpressing cells (1.5-fold over WT and vector control;

$B_f = 0.5$ and 0.4 , respectively, Fig. 5A), consistent with 8-oxoG being a major oxidized lesion. Moreover, a higher mtOgg1 overexpression (2.7-fold over vector control) resulted in essentially complete protection against MQ-induced mtDNA damage (B_f of 0.5 and 0.01 in vector control and Ogg1 overexpressers, respectively, Fig. 5B). This correspondence of attenuated mtDNA damage with mtOgg1 overexpression suggests that elevated mtOgg1 probably prevented further mtDNA damage and allowed for complete repair.

Inhibition of GSH synthesis and mtGSH transport exacerbates MQ-induced mtDNA damage

Given the role of cytosolic GSH in controlling mtGSH homeostasis [35], we tested the influence of an altered cytosolic GSH pool in MQ-induced mtDNA damage by inhibiting cytosolic GSH synthesis with BSO. The results in Fig. 6A show that BSO at 5 and 20 μM dose-dependently decreased cytosolic GSH without significantly altering GSSG levels, consistent with diminished GSH synthesis. In comparison, only 20 μM BSO induced significant decreases in mtGSH (Fig. 6B), indicating that mild reduction in cytosolic GSH synthesis with 5 μM BSO did not adversely alter mtGSH status. As with cytosolic GSSG, BSO at 5 and 20 μM exerted minimal effects on mtGSSG (Fig. 6B). In accordance with BSO-induced decreases in cytosolic and mitochondrial GSH, we found an exacerbation of mtDNA damage in BSO-treated cells caused by 30 min exposure to 100 μM MQ ($B_f = 1.1$ and 1.4 for 5 and 20 μM BSO compared to $B_f = 0.4$ in the absence of BSO) (Fig. 7A). Cytosolic GSH was dose-dependently lower in BSO-treated cells challenged with MQ compared to non-BSO-treated cells (Fig. 7B,

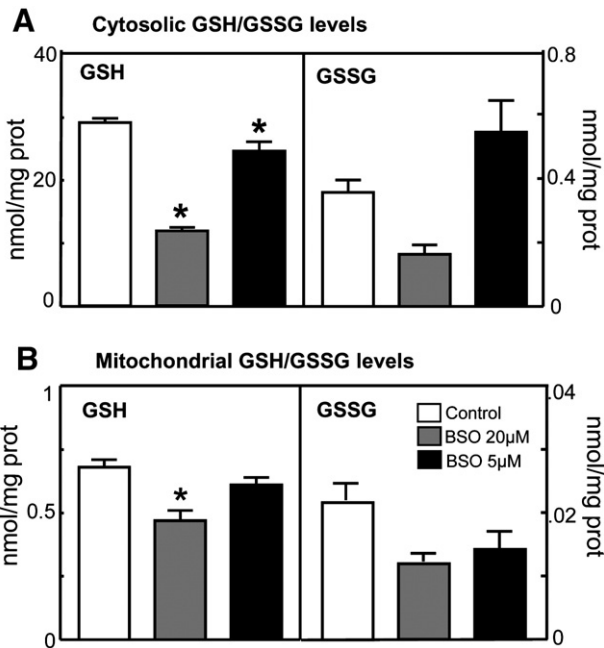


Fig. 6. Effects of BSO inhibition of GSH synthesis on cytosolic and mitochondrial GSH and GSSG status. NCM460 cells were exposed to 100 μM MQ for 30 min without or with pretreatment for 24 h with BSO (5 or 20 μM). GSH and GSSG concentrations in the cytosolic and mitochondrial compartments were determined after digitonin fractionation as described under Materials and methods. Results are expressed as nmol/mg protein and presented as means ± SE of three separate experiments performed in duplicates. (A) Cytosolic GSH and GSSG; (B) mitochondrial GSH and GSSG. In each instance, * $P < 0.05$ versus untreated control.

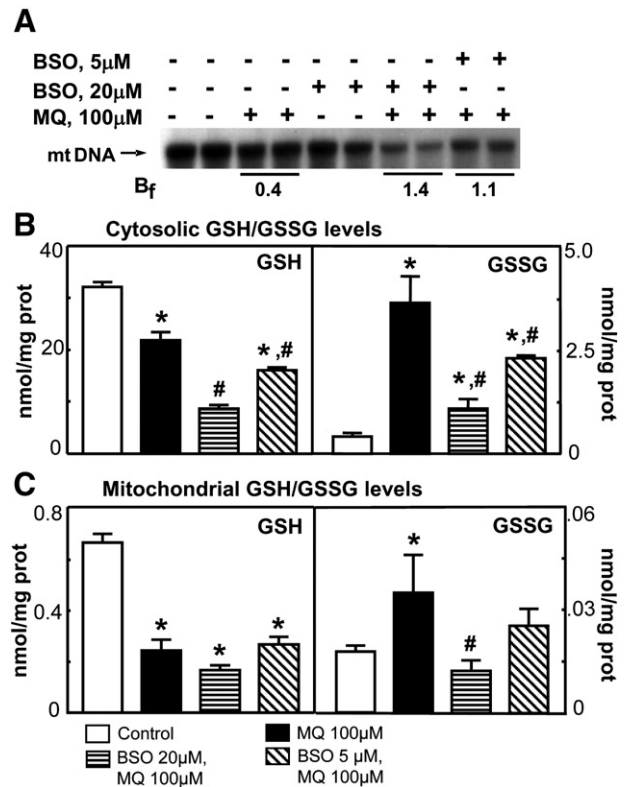


Fig. 7. Inhibition of GSH synthesis exacerbates MQ-induced mtDNA damage in association with decreased cytosolic and mitochondrial GSH. NCM460 cells were exposed to 100 μM MQ for 30 min without or with pretreatment for 24 h with BSO (5 or 20 μM). (A) Total DNA was extracted and probed for mtDNA by Southern blot. mtDNA damage is expressed as strand B_f and one representative of three gels is shown. GSH and GSSG concentrations were determined in the (B) cytosol and (C) mitochondria after digitonin permeabilization. Results are expressed as nmol/mg protein and presented as means ± SE of three separate experiments performed in duplicates. In each instance, * $P < 0.05$ versus untreated control; # $P < 0.05$ versus MQ alone.

left). Total cytosolic GSSG levels were also decreased in these cells (Fig. 7B, right), consistent with overall reduction in cellular GSH due to inhibition of synthesis. MQ induced significant mtGSSG formation (Fig. 7C, right) and a 60% decrease in mtGSH (Fig. 7C, left), a greater loss than cytosolic GSH under these conditions. Interestingly, BSO treatment did not result in further decrease in mtGSH (Fig. 7C, left), suggesting that maximal mtGSH depletion was already achieved by MQ challenge. Consistent with the inhibition of GSH synthesis and overall decrease in total cytosolic GSH, the mitochondrial GSH pool (GSH plus GSSG) was lower than in non-BSO-treated cells regardless of MQ exposure (Fig. 7C). Collectively, these results indicate that maintenance of the cytosolic GSH pool is important in mtDNA protection. The protective mechanism is consistent with the role of cytosolic GSH in maintaining mitochondrial GSH supply.

Because the cytosolic GSH pool is critical in supporting normal mtGSH status through mtGSH uptake, we investigated the contribution of mtGSH transport and mitochondrial matrix GSH to MQ-induced mtDNA damage. MtGSH uptake was manipulated by pharmacological or genetic means. Combined inhibition of DIC and OGC carriers by BM and PS, respectively, enhanced mtDNA damage induced by 30 min exposure to 100 μ M MQ (Fig. 8A, lanes 2 and 4). Interestingly, treatment of cells with combined BM/PS alone caused some mtDNA damage, which was exacerbated by MQ (Fig. 8A, lanes 3 and 4). The small extent of damage to mtDNA by BM/PS alone suggests some perturbation of basal mitochondrial function, consistent with our recent finding that BM/PS caused a measurable, albeit insignificant, decrease in cellular ATP; however, BM/PS per se did not induce NCM460 cell apoptosis in the absence of MQ [20]. Collectively, the results demonstrate that compromised mtGSH transport enhances mtDNA susceptibility, which can be exacerbated by oxidative challenge.

To further define a role for mtGSH transport, MQ-induced mtDNA damage was examined in HT-29 cells that stably overexpress the wild-type OGC carrier. HT-29 cells were treated with 100 μ M MQ for 1 h, because these cells were more resistant to MQ [20]. The results in Fig. 8B show that MQ induced substantial mtDNA damage in parent (WT) HT-29 cells ($B_f=0.4$), which was exacerbated by inhibition of mtGSH transport with BM/PS ($B_f=0.7$), responses that were similar to those of NCM460 cells (Fig. 8A). In contrast, mtDNA was protected against MQ challenge in HT-29 clones that overexpress the WT-OGC transporter ($B_f=0.05$; Fig. 8C), indicating that upregulation of the OGC carrier for increased mtGSH uptake effectively conferred protection of mtDNA against oxidative stress. Taken together, these

results support our hypothesis that mtGSH transport is an important contributor to mtDNA preservation during oxidative challenge.

Discussion

The results of this study provide evidence that oxidative damage to mtDNA and its recovery are sensitive to cell GSH; notably the mtGSH pool plays an important role in preserving mtDNA integrity during oxidative stress. Our conclusion is supported by several lines of evidence. First, MQ elicited oxidative mtDNA damage that was associated with increased mitochondrial and cytosolic GSSG and mitochondrial protein disulfide and was prevented by NAC, indicating that mtDNA damage is redox sensitive. Second, inhibition of GSH synthesis with BSO exacerbated mtDNA damage in accordance with decreased cytosolic GSH and mtGSH, which supports a role for cytosolic GSH in preserving mtGSH and mtDNA. Significantly, the blockade of mtGSH transport by pharmacologic agents exaggerated mtDNA damage, which was prevented by overexpression of the mtGSH transporter OGC, thus underscoring the importance of cytosol-to-mitochondria GSH import in mtDNA integrity. These findings collectively support our central hypothesis that mtGSH is a pivotal player in MQ-mediated mtDNA damage. Finally, postoxidative recovery of mtDNA was preceded by restored baseline GSH levels, suggesting that cellular GSH status not only impacts oxidant-mediated mtDNA damage, but additionally could influence its repair.

Our finding that the oxidation of the cytosolic and mitochondrial GSH compartments preceded MQ-induced mtDNA damage is consistent with a temporal link between disruption of cellular GSH homeostasis and vulnerability of mtDNA to oxidative challenge. However, preferential oxidation of mitochondrial proteins by MQ suggests that impairment of mitochondrial redox balance could have a greater impact on the level of mtDNA damage during oxidative stress. A direct relationship between mtGSH and mtDNA damage was supported by the findings that blockade of mtGSH uptake potentiated, whereas overexpression of mtGSH OGC carrier nullified, the effect of MQ on mtDNA damage (Fig. 8). Because mitochondria are implicated as major sites for quinone redox cycling [20], mitochondria-derived ROS would elicit a mtGSH redox imbalance and consequent oxidative injury to mtDNA. Previous studies have shown that the depletion of mtGSH by diethyl maleate to 70–80% of the control value potentiated radiation-induced mtDNA damage [36] and that oxidation of mtGSH increased age-associated levels of 8-oxoG in mice and rats [37]. In hepatocytes isolated from hemin-treated rats, a decrease in mtGSH after exposure to *t*-BH was associated with a rapid increase in mtDNA deletion, a marker of oxidative damage [38]. Interestingly, in isolated rat mitochondria, Giulivi and Cadenas [39] demonstrated that an increase in mtDNA oxidation as measured by 8-oxoG was associated with elevated mtGSH. The authors concluded that mtGSH can function as an electron donor in DNA oxidation because of the presence Cu^{2+} in the incubation reaction [39]. Thus, the significance of the findings in isolated mitochondria regarding the central role of mtGSH in oxidative mtDNA damage or mtDNA protection in cells is unclear. However, it is clear from the current study that in colonic epithelial cells, mtGSH is critical for the protection of mtDNA against oxidative stress.

The result that NAC was highly effective in protection against oxidative mtDNA damage underscores a redox mechanism in mtDNA damage. The mechanism of how mtGSH influences oxidative mtDNA damage is unresolved. Our results suggest that mtGSH oxidation is likely to be a key contributor to the formation of mtDNA oxidative lesions. Consistent with this interpretation, NAC protection against mtDNA damage was correlated with significant attenuation in mtGSSG; interestingly, NAC did not completely restore the mitochondrial GSH/GSSG redox imbalance (Fig. 4B), indicating a nonlinear relationship between oxidative mtDNA damage and the mtGSH redox state. It is possible that oxidative damage to mtDNA occurred when

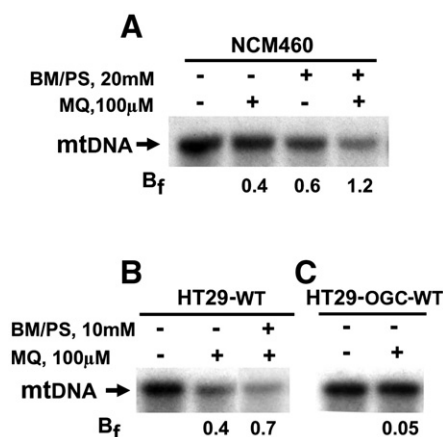


Fig. 8. MQ-induced mtDNA damage correlates with mtGSH transport. (A) NCM460 or (B) HT-29 cells were exposed to 100 μ M MQ for 30 min without or with pretreatment for 1 h with BM/PS (20 mM). (C) HT-29 cells overexpressing the OGC carrier were exposed to 100 μ M MQ for 30 min. In each instance, total DNA was extracted and mtDNA was quantified by Southern blot analysis as described under [Materials and methods](#). mtDNA damage is expressed as strand B_f . One representative of three gels is shown.

the mtGSH/GSSG redox status fell below a critical threshold level and that NAC, by attenuating mtGSSG formation, maintained the redox status above this threshold. Alternatively, the extent of oxidative mtDNA damage may also be a direct result of the increase in mtGSSG, which NAC effectively prevented. Thus, by attenuating mtGSSG, NAC could function to lower the oxidative burden on the mitochondria and thereby preserve mtDNA integrity. Interestingly, GSH oxidation was not correlated with basal (steady-state) levels of DNA base modification in a variety of mammalian cell types in the absence of oxidative challenge [40]. Indeed, in A52 Chinese hamster cells the administration of NAC or cysteine ester not only did not prevent basal damage to DNA, but seemed to promote base oxidation [40].

Generally, the maintenance of a reduced mtGSH redox environment would favor mtDNA protection, given the role of mtGSH in quenching mitochondria-derived ROS. Additionally, mtGSH could influence mtDNA repair. A possible connection between mtGSH and post-MQ repair of mtDNA is suggested by the rapid recovery of cytosolic and mitochondrial GSH to preoxidant levels that preceded mtDNA recovery (Fig. 3). Precisely what role mtGSH plays in the repair process is unclear. One possibility is that mtGSH modulates the function of mtDNA repair enzymes. Oxidatively damaged mtDNA is recognized and removed by mtBER enzymes. Among the main mammalian DNA glycosylases [41], Ogg1 cleaves 8-oxoG [9]. Our results show that the overexpression of mtOgg1 afforded significant protection against MQ-induced oxidative mtDNA damage, indicating that 8-oxoG was, in fact, a major oxidative by-product. Previous studies have similarly demonstrated the protection of mtDNA from damage induced by high levels of MQ (400 μ M) in mtOgg1-overexpressing HeLa cells [31] that was associated with increased mtOgg1 repair activity [34]. The age-associated decrease in mtOgg1 activity [42] and its mitochondrial localization [43] suggest that increased oxidative stress would comprise both the efficiency and the capacity for the repair of oxidized mtDNA. Ongoing studies are examining the effects of mtGSH redox status on mtOgg1 activity and whether GSH-dependent S-glutathionylation is important as a posttranslational mechanism for the regulation of mtOgg1 and other important repair enzymes.

The importance of the cytosolic GSH compartment in mtDNA preservation is notable as reflected in its capacity to preserve the mt-matrix GSH pool. The exacerbation of MQ-induced mtDNA damage by inhibition of de novo cytosolic GSH synthesis (Fig. 7) is consistent with a crucial role for cytosolic GSH in mtGSH homeostasis and the protection of mtDNA against oxidant challenge. In agreement, previous studies have reported an exacerbation of oxidative DNA damage after GSH depletion with BSO [44,45]. Moreover, Hollins et al. demonstrated that decreased cellular GSH levels in lymphocytes exposed to *t*-BH were correlated with increases in ROS and mtDNA modification, measured as changes in mtDNA copy number and a 4977-bp deletion from the mitochondrial genome [46]. In other studies, in 3Y1 fibroblasts in vitro and in rat mammary gland in vivo, the oxidation of cellular GSH was found to precede nuclear DNA fragmentation, suggesting a possible link between cellular GSH and nuclear DNA damage.

The significance of mtGSH in colonic cell survival is underscored by our recent findings that the preservation of mtGSH transport and hence mt-matrix GSH is critical to protecting NCM460 cells against MQ challenge and promoting cell survival [20]. Specifically, the maintenance of a reduced mtGSH redox environment was essential in preserving mitochondrial ATP production and the mitochondrial membrane potential [20]. Importantly, the current study demonstrates that mtGSH also functions in the protection of mtDNA integrity, particularly during oxidative challenge. The biological consequence of oxidative mtDNA damage in cell apoptosis has been demonstrated by LeDoux and co-workers [31]. Precisely how damaged mtDNA signals cell apoptosis during acute oxidative challenge is not completely understood. One possibility may be

related to apoptotic signaling via enhanced superoxide generation secondary to mtDNA damage and mitochondrial failure resulting from decreased expression of mitochondrial genome-encoded respiratory proteins. In support of this scenario, recent studies demonstrated that ROS-mediated oxidative mtDNA damage can signal cellular apoptosis by causing impairment of mitochondrial protein expression, complex I dysfunction, and increased ROS production that ultimately triggered the collapse of the mitochondrial membrane potential [47]. Previous studies have also implicated enhanced ROS formation in apoptotic signaling induced by oxidatively damaged mtDNA [48], but its quantitative importance as a major mechanism in oxidative cell killing remains to be validated.

Acknowledgment

This study was supported by Grant DK44510 from the National Institutes of Health.

References

- [1] Yakes, F. M.; Van Houten, B. Mitochondrial DNA damage is more extensive and persists longer than nuclear DNA damage in human cells following oxidative stress. *Proc. Natl. Acad. Sci. USA* 94:514–519; 1997.
- [2] Richter, C.; Park, J. W.; Ames, B. N. Normal oxidative damage to mitochondrial and nuclear DNA is extensive. *Proc. Natl. Acad. Sci. USA* 85:6465–6467; 1988.
- [3] Klungland, A.; Rosewell, I.; Hollenbach, S.; Larsen, E.; Daly, G.; Epe, B.; Seeburg, E.; Lindahl, T.; Barnes, D. E. Accumulation of premutagenic DNA lesions in mice defective in removal of oxidative base damage. *Proc. Natl. Acad. Sci. USA* 96:13300–13305; 1999.
- [4] Ballinger, S. W.; Patterson, C.; Yan, C. N.; Doan, R.; Burow, D. L.; Young, C. G.; Yakes, F. M.; Van Houten, B.; Ballinger, C. A.; Freeman, B. A.; Runge, M. S. Hydrogen peroxide- and peroxynitrite-induced mitochondrial DNA damage and dysfunction in vascular endothelial and smooth muscle cells. *Circ. Res.* 86:960–966; 2000.
- [5] Ide, T.; Tsutsui, H.; Hayashidani, S.; Kang, D.; Suematsu, N.; Nakamura, K.; Utsumi, H.; Hamasaki, N.; Takeshita, A. Mitochondrial DNA damage and dysfunction associated with oxidative stress in failing hearts after myocardial infarction. *Circ. Res.* 88:529–535; 2001.
- [6] Ozawa, T. Oxidative damage and fragmentation of mitochondrial DNA in cellular apoptosis. *Biosci. Rep.* 17:237–250; 1997.
- [7] LeDoux, S. P.; Wilson, G. L.; Beecham, E. J.; Stevnsner, T.; Wassermann, K.; Bohr, V. A. Repair of mitochondrial DNA after various types of DNA damage in Chinese hamster ovary cells. *Carcinogenesis* 13:1967–1973; 1992.
- [8] LeDoux, S. P.; Wilson, G. L. Base excision repair of mitochondrial DNA damage in mammalian cells. *Prog. Nucleic Acid Res. Mol. Biol.* 68:273–284; 2001.
- [9] Nishimura, S. Involvement of mammalian OGG1(MMH) in excision of the 8-hydroxyguanine residue in DNA. *Free Radic. Biol. Med.* 32:813–821; 2002.
- [10] Henle, E. S.; Linn, S. Formation, prevention, and repair of DNA damage by iron/hydrogen peroxide. *J. Biol. Chem.* 272:19095–19098; 1997.
- [11] Hamilton, M. L.; Van Remmen, H.; Drake, J. A.; Yang, H.; Guo, Z. M.; Kewitt, K.; Walter, C. A.; Richardson, A. Does oxidative damage to DNA increase with age? *Proc. Natl. Acad. Sci. USA* 98:10469–10474; 2001.
- [12] Stuart, J. A.; Brown, M. F. Mitochondrial DNA maintenance and bioenergetics. *Biochim. Biophys. Acta* 1757:79–89; 2006.
- [13] Harrison, J. F.; Hollensworth, S. B.; Spitz, D. R.; Copeland, W. C.; Wilson, G. L.; LeDoux, S. P. Oxidative stress-induced apoptosis in neurons correlates with mitochondrial DNA base excision repair pathway imbalance. *Nucleic Acids Res.* 33:4660–4671; 2005.
- [14] Meredith, M. J.; Reed, D. J. Status of the mitochondrial pool of glutathione in the isolated hepatocyte. *J. Biol. Chem.* 257:3747–3753; 1982.
- [15] Hallberg, E.; Rydstrom, J. Selective oxidation of mitochondrial glutathione in cultured rat adrenal cells and its relation to polycyclic aromatic hydrocarbon-induced cytotoxicity. *Arch. Biochem. Biophys.* 270:662–671; 1989.
- [16] Lluís, J. M.; Morales, A.; Blasco, C.; Colell, A.; Mari, M.; Garcia-Ruiz, C.; Fernandez-Checa, J. C. Critical role of mitochondrial glutathione in the survival of hepatocytes during hypoxia. *J. Biol. Chem.* 280:3224–3232; 2005.
- [17] Olafsdottir, K.; Reed, D. J. Retention of oxidized glutathione by isolated rat liver mitochondria during hydroperoxide treatment. *Biochim. Biophys. Acta* 964:377–382; 1988.
- [18] Fernandez-Checa, J. C.; Garcia-Ruiz, C.; Ookhtens, M.; Kaplowitz, N. Impaired uptake of glutathione by hepatic mitochondria from chronic ethanol-fed rats: tracer kinetic studies in vitro and in vivo and susceptibility to oxidant stress. *J. Clin. Invest.* 87:397–405; 1991.
- [19] Zhao, P.; Kalhorn, T. F.; Slattery, J. T. Selective mitochondrial glutathione depletion by ethanol enhances acetaminophen toxicity in rat liver. *Hepatology* 36:326–335; 2002.
- [20] Circu, M. L. R. C.; Maloney, R.; Moyer, P. M.; Aw, T. Y. Contribution of mitochondrial GSH transport to matrix GSH status and colonic epithelial cell apoptosis. *Free Radic. Biol. Med.* 44:768–778; 2008.
- [21] Chen, Z.; Lash, L. H. Evidence for mitochondrial uptake of glutathione by dicarboxylate and 2-oxoglutarate carriers. *J. Pharmacol. Exp. Ther.* 285:608–618; 1998.

- [22] Chen, Z.; Putt, D. A.; Lash, L. H. Enrichment and functional reconstitution of glutathione transport activity from rabbit kidney mitochondria: further evidence for the role of the dicarboxylate and 2-oxoglutarate carriers in mitochondrial glutathione transport. *Arch. Biochem. Biophys.*